

# Frequency Response of a Fractional Order Shunt Resonator of the Class $R-RL_{\beta}C_{\alpha}$

Mehmet Emir Koksall

Department of Mathematics, Ondokuz Mayıs University, Samsun, Turkey  
 Email: mekoksall@omu.edu.tr

**Abstract**—Frequency domain analysis of a fractional order parallel shunt resonator of the class  $R-RL_{\beta}C_{\alpha}$  is conducted. The voltage and current waveforms are computed in the frequency domain. It is shown that the circuit exhibits all three types of basic filtering characteristics; namely low-pass, band-pass, and high-pass.

**Keywords**—Fractional order derivative, frequency response, fractional inductance, fractional capacitance.

## I. INTRODUCTION

Although the fractional order (FO) derivative is not new in mathematics [1], it has gained great popularity in the application of fractional calculus in the last few decades at various areas of science and engineering [2-7]. In particular, electrical circuits having FO components have been dealt with many authors [8-11]. In [12], Walczak and Jacubowska studied the series FO  $RL_{\beta}C_{\alpha}$  circuit. And a recent paper by Ciszek and Walczak has covered the transients states of a parallel circuit composed of fractional order inductor and capacitor branches are analyzed.

Ciszek and Walczak presented the results of transient analysis in a parallel circuit containing a real coil  $L_{\beta}$  and a supercapacitor  $C_{\alpha}$  modelled as fractional elements in their paper [13]. Current and voltage waveforms are obtained with different current source excitations for both cases of real and complex poles. But they hardly concerned with the frequency response characteristics of the circuit. In this contribution, we study the frequency response characteristics of the similar circuit but added with a load resistance  $R$  which can be treated as (or combined with) the source resistance as well. The resulting circuit is shortly denoted by  $R-RL_{\beta}C_{\alpha}$ , and as far as the author's knowledge, it has not been studied before.

The paper is organized as follows; Section 2 introduces the  $R-RL_{\beta}C_{\alpha}$  circuit and its formulation. Section 3 covers the derivation of the transfer functions. Frequency response properties and time domain step responses are studied on the base of examples in Section 4. Finally, Section 5 covers the conclusions.

## II. $R-RL_{\beta}C_{\alpha}$ CIRCUIT

The FO parallel resonator circuit considered in this paper is shown in Fig. 1. The FO coil inductance is  $L_{\beta}$  and FO capacitance is  $C_{\alpha}$ ;  $\alpha, \beta \in R^+$ .  $R_L$  is the series internal resistance of the coil,  $R_C$  is the ESR resistance of the capacitor. The circuit is excited by a parallel current source  $I(t)$ ;  $R$  represents either the internal resistance of the source and/or the load resistance of the circuit, if both exist they can be combined.  $I_R, I_L, I_C$  represent currents flowing through the resistor, inductor, and capacitor respectively. According to the Kirchhoff's current law

$$I_R(t) + I_L(t) + I_C(t) = I(t). \quad (1)$$

The component behavior equations are

$$V = RI_R, V_{RL} = R_L I_L, V_{RC} = R_C I_C, \quad (2a, b, c)$$

for the resistances. The FO components are modelled by

$$V_{L_{\beta}}(t) = L_{\beta} \frac{d^{\beta} I_L(t)}{dt^{\beta}}, I_C(t) = C_{\alpha} \frac{d^{\alpha} V_{C_{\alpha}}(t)}{dt^{\alpha}}. \quad (3a, b)$$

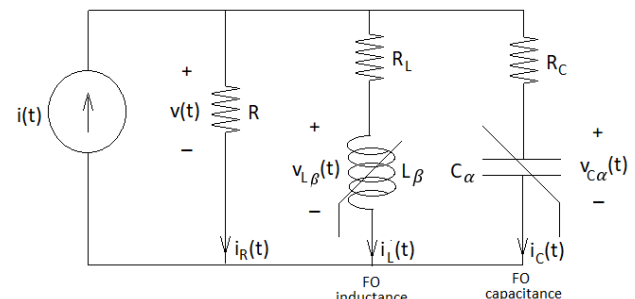


Fig. 1: Fractional order shunt resonator

## III. TRANSFER FUNCTIONS

From the Kirchhoff's voltage law

$$V(t) = R_L I_L(t) + V_{L_{\beta}}(t), \quad (4a)$$

$$V(t) = R_C I_C(t) + V_{C_{\alpha}}(t). \quad (4b)$$

Taking the Laplace transform of Eqs. (1-4) with zero critical conditions, we obtain

$$I_R + I_L + I_C = I, \quad (5)$$

$$V = RI_R, V_{RL} = R_L I_L, V_{RC} = R_C I_C, \quad (6a, b, c)$$

$$V_{L_{\beta}} = L_{\beta} S^{\beta} I_L, I_C = C_{\alpha} S^{\alpha} V_{C_{\alpha}}, \quad (7a, b)$$

$$V = R_L I_L + V_{L_{\beta}}, V = R_C I_C + V_{C_{\alpha}}. \quad (8a, b)$$

These eight equations in eight unknowns ( $I_R, I_L, I_C, V, V_{RL}, V_{RC}, V_{L_{\beta}}, V_{C_{\alpha}}$ ) can be solved in terms of  $I$ ; the resulting transfer functions are

$$H_{VR} = \frac{V}{I} = \frac{\Delta_v(s)}{\Delta(s)}, \quad (9a)$$

$$H_{IR} = \frac{I_R}{I} = \frac{\Delta_v(s)}{R\Delta(s)}, \quad (9b)$$

$$H_{IL} = \frac{I_L}{I} = \frac{\Delta_v(s)}{(L_\beta S^\beta + R_L)\Delta(s)}, \quad (9c)$$

$$H_{IC} = \frac{I_C}{I} = \frac{C_\alpha S^\alpha \Delta_v(s)}{(R_C C_\alpha S^\alpha + 1)\Delta(s)}, \quad (9d)$$

$$H_{VL} = \frac{V_{L\beta}}{I} = \frac{L_\beta S^\beta \Delta_v(s)}{(L_\beta S^\beta + R_L)\Delta(s)}, \quad (9e)$$

$$H_{VC} = \frac{V_{C\alpha}}{I} = \frac{\Delta_v(s)}{(R_C C_\alpha S^\alpha + 1)\Delta(s)}, \quad (9f)$$

$$H_{VRL} = \frac{V_{RL}}{I} = R_L \frac{I_L}{I} = \frac{R_L \Delta_v(s)}{(L_\beta S^\beta + R_L)\Delta(s)}, \quad (9g)$$

$$H_{IRC} = \frac{V_{RC}}{I} = R_C \frac{I_C}{I} = \frac{R_C C_\alpha S^\alpha \Delta_v(s)}{(R_C C_\alpha S^\alpha + 1)\Delta(s)}. \quad (9h)$$

Where, with  $\mu = \frac{1}{GR_C + 1}$ ,  $\eta = GR_L + 1$ ,  $G = \frac{1}{R}$ ,

$$\Delta_v(s) = \mu \left( R_L S^{\alpha+\beta} + \frac{R_L R_C}{L_\beta} S^\alpha + \frac{1}{C_\alpha} S^\beta + \frac{R_L}{L_\beta C_\alpha} \right),$$

$$\Delta(s) = S^{\alpha+\beta} + \frac{R_C}{L_\beta} \left( \mu + \frac{R_L}{R_C} \right) S^\alpha + \frac{\mu G}{C_\alpha} S^\beta + \frac{\mu \eta}{L_\beta C_\alpha}.$$

From (6), the FO differential equation governing the dynamics of the circuit can be obtained by replacing the Laplace operator  $S^\gamma$  with  $\frac{d^\gamma}{dt^\gamma}$ , the result is

$$\begin{aligned} & \frac{d^{\alpha+\beta}}{dt^{\alpha+\beta}} v + \frac{R_C}{L_\beta} \left( \mu + \frac{R_L}{R_C} \right) \frac{d^\alpha}{dt^\alpha} v + \frac{\mu G}{C_\alpha} \frac{d^\beta}{dt^\beta} v + \frac{\mu \eta}{L_\beta C_\alpha} v \\ &= \mu R_L \frac{d^{\alpha+\beta}}{dt^{\alpha+\beta}} I + \frac{\mu R_L R_C}{L_\beta} \frac{d^\alpha}{dt^\alpha} I + \frac{\mu}{C_\alpha} \frac{d^\beta}{dt^\beta} I + \frac{\mu R_L}{L_\beta C_\alpha} I. \end{aligned} \quad (10)$$

Since the scope of the paper is mainly confined to frequency response characteristics, the solution of this fractional order differential equation for  $v(t)$  when different types of excitons (such as impulse, step, sinusoid etc.) is left as a future work. The result will be the generalization of the analytical solutions given in [13] for the case of nonideal current source and/or the existence of a load resistance in the circuit.

#### IV. EXAMPLES

As the first example, assume the numerical values of the components are chosen as follows: a supercapacitor of pseudo-capacitance  $C_\alpha = 10F/s^{1-\alpha}$ , with a series internal resistance of  $R_C = 0.1\Omega$ ; a real FO coil of pseudo-inductance  $L_\beta = 1 + s^{1-\beta}$  with a series interval resistance of  $R_L = 0.1\Omega$ . Coefficients of the FO elements are  $\alpha = 0.5, \beta = 0.25$ . The source and/or load resistance  $R = 4\Omega$ .

The Bode plots of transfer functions  $H_{IR}, H_{IL}, H_{IC}$  are shown in Fig. 2. It is seen that  $H_{IL}$  ( $H_{IC}$ ) exhibits low pass (high pass) filter characteristics, and  $H_{IR}$  has a small magnitude of type band pass, which is due to the

relatively high value of  $R = 4\Omega$ . The gain and phase relations are observed to be consistent with Eqs. (9b,c,d).

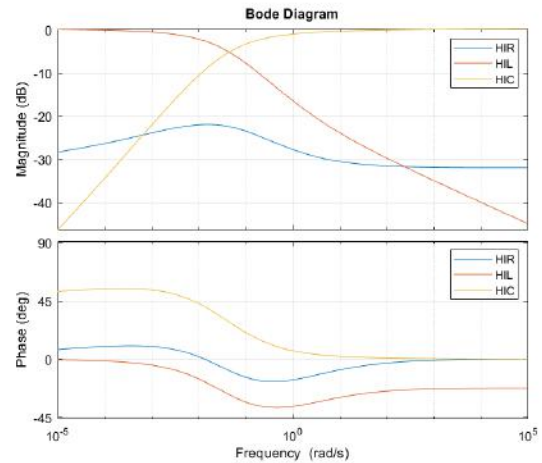


Fig. 2: Bode Plots of  $H_{IR}, H_{IL}, H_{IC}$  for Example 1

Fig. 3 shows the time variations of the currents  $I_{L\beta}, I_{C\alpha}, I_R$ . It is observed that  $I_R$  is smaller than  $I_{L\beta}$  and  $I_{C\alpha}(t)$  due to high values of  $R$ .  $I_{L\beta}$  and  $I_{C\alpha}(t)$  show step responses typical to low pass and high pass filters, respectively. Note also that these three characteristics sum up to unity at any time.

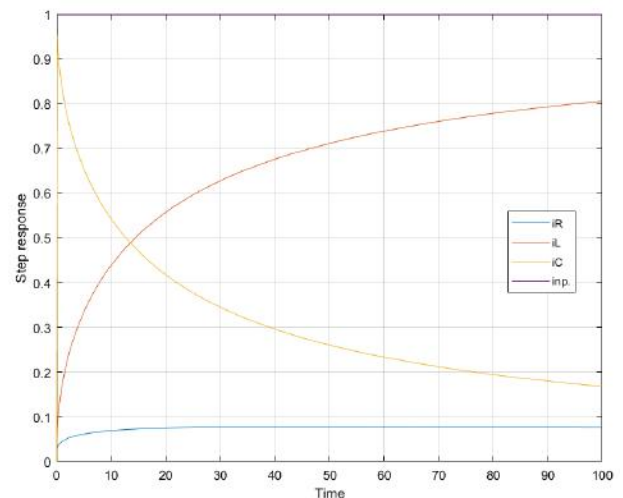


Fig. 3: Step Responses for the Currents in Example 1

Step response for the voltages  $V_R, V_{RL}, V_L, V_{RC}, V_C$  are shown in Fig. 4. Note that Kirchhoff's voltage laws  $V_{RL} + V_L = V_R, V_{RC} + V_C = V_R$  are satisfied.

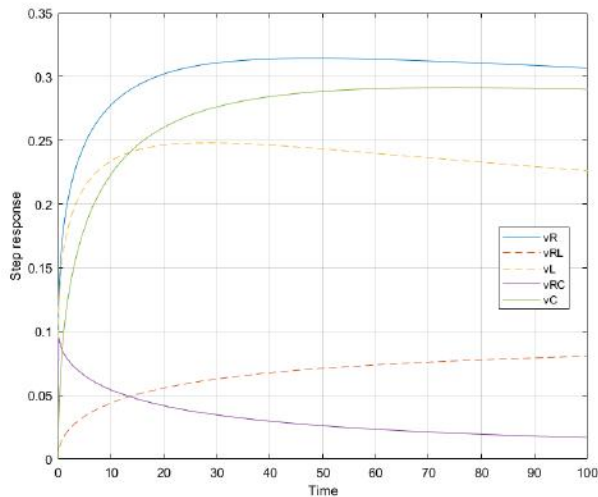
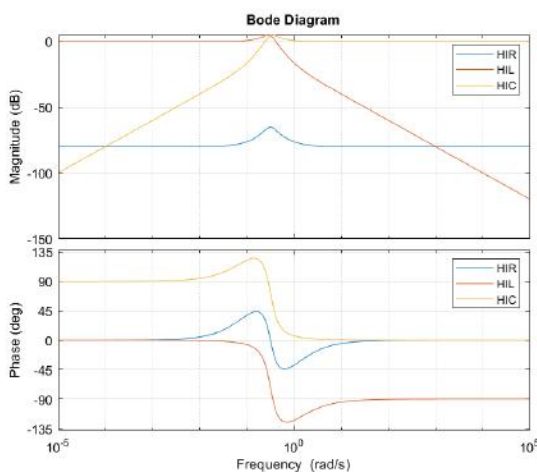


Fig. 4: Step Responses for the Voltages in Example 1

The hole circuit exhibits an overdamped type step response characteristics and highly stable.

As the second example, we consider the same parameters values except,  $\beta = 1.00$ ,  $\alpha = 1.00$  and  $R = 1000\Omega$ . This case corresponds to an integer order circuit with a very slight load  $R$ , whilst the internal losses  $R_L$  and  $R_C$  are present.

The results of the simulations are presented in Figs. 5,6,7. In Fig. 5, the low pass and high pass characteristics of  $H_{IL}$  and  $H_{IC}$  are preserved, but the cut off rate is sharper. It is also apparent that  $H_{IR}$  is much more reduced than in Example 1 due to the high resistance  $R = 1000\Omega$ , though it is still a band pass characteristic. The same sharpening is observed in the phase characteristics as well.

Fig. 5: Bode Plots of  $H_{IR}$ ,  $H_{IL}$ ,  $H_{IC}$  for Example 2

Currents  $I_R$ ,  $I_{L\beta}$ ,  $I_{C\alpha}$  for a unit step are plotted in Fig. 6. It is seen that  $V_R(t)$  is almost zero since  $R = 1000\Omega$ . Further, the currents  $I_R$ ,  $I_{L\beta}$ ,  $I_{C\alpha}$  sum up to the unit input step. The circuit behaves as an underdamped circuit due

to oscillations in the responses. The damping is small due to the small values of internal resistances  $R_L$  and  $R_C$ .

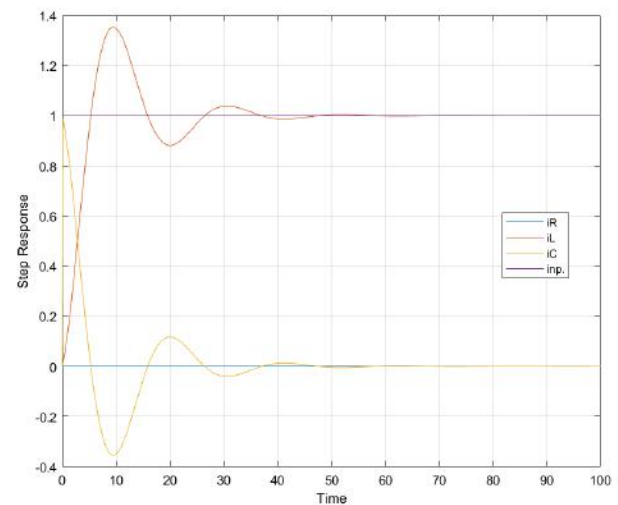


Fig. 6: Step Responses for the Currents in Example 2

Step responses for the voltages  $V_R$ ,  $V_{RL}$ ,  $V_L$ ,  $V_{RL}$  and  $V_C$  are shown in Fig. 7. The underdamped nature of the circuit is observed in all responses. Kirchhoff's voltage laws  $V_{RL} + V_L = V_R$ ,  $V_{RC} + V_C = V_R$  are still observed in all responses.  $V_{RC}$  goes to 0 as  $t$  gets large due to open circuit behavior of the capacitor under steady-state conditions with step input so it hardly passes current, so that  $V_{RC} = 0$ .

Similar argument holds for the inductor; it behaves as short circuit under step input steady-state conditions and the voltage across  $R_{L\beta}$  is generated by the full input current, so  $V_{RL\beta} = R_{L\beta} \cdot 1 = 0.1A$  as  $t$  gets infinity.

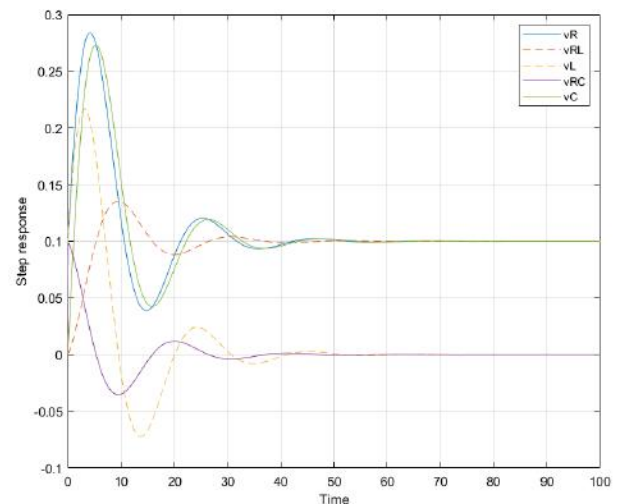


Fig. 7: Step Responses for the Voltages in Example 2.

## V. CONCLUSION

Frequency response characteristics and step responses of a lossy, fractional order, parallel  $RLC$  circuit driven by a current source is investigated in this paper. Since the circuit is loaded and/or driven by a non-ideal current source due to its internal resistance, it is denoted by the

class  $RL_{\beta}C_{\alpha}$ , where the first  $R$  denotes this resistance. The circuit is modelled in both time and frequency domains, but only frequency domain analysis results are given. Three types of filter characteristics are noted each of which due to a branch of the circuit. It is observed that the circuit exhibits the response characteristics of a tank resonator with lossy capacitor and inductor for unity values of the fractional orders. It is avoided from further numerical examples to keep the content substantial. Explicit solutions of different voltages and currents in the circuit when it is excited by several types of source waveforms (such as step, sinusoidal, exponential, poly-harmonic and arbitrary being an element of a Hilbert space) can be found by the Laplace transform method applying the decomposition of FO rational functions to partial fractions. The results will involve single and two parameter Mittag-Leffler function. However, due to the added source and/or load resistance  $R$ , the characteristic polynomial gets more complicated and this will cover much more effort than in [13]. Therefore, that part of the study is left as a future work.

#### REFERENCES

- [1] I. Podlubny, Fractional Differential Equations, Academic Press, 1999.
- [2] L. Zhang, Y. Yang, F. Wang, "Synchronization analysis of fractional-order neural networks with time-varying delays via discontinuous neuron activations", Neuroscience, vol. 275, pp. 40-49, 2018.
- [3] V. Wesh, A. Vyawahare, G.E. Paredes, "On the stability of linear fractional-space neutron kinetics (F-SNPK) models for nuclear reactor dynamics", Annuals of Nuclear Energy, vol. 111, pp. 12-21, 2018.
- [4] H. Singh, "Approximate solutions of fractional vibration equation using Jacobi polynomials", Applied Mathematics and Computation, vol. 317, pp. 85-100, 2018.
- [5] A. Dabiri, M. Poursina, E. Butcher, M. Nazari, "Optimal Periodic-Gain Fractional Delayed State Feedback Control for Linear Fractional Periodic Time-Delayed Systems", April 2018, IEEE Transactions on Automatic Control PP(99), DOI: 10.1109/TAC.2017.2731522.
- [6] D. Bouagadaa, S. Melchiorb, P.V. Dooren, "Calculating the  $H_{\infty}$  norm of a fractional system given in state-space form", Applied Mathematics Letters, vol. 79, pp. 51-57, 2018.
- [7] L. Marinangeli, F. Alijani, S.H. Hosseina, "Fractional-order positive position feedback compensator for active vibration control of a smart composite plat", Journal of Sound and Vibration, vol. 412, pp. 1-16, 2017.
- [8] F. Gomez, J. Rosales, M. Guia, "RLC electrical circuits of non-integer order", Central European Journal of Physics, vol. 11, pp. 1361-1365, 2013.
- [9] J.F. Gomez-Aguilar, A. Atangana, V.F. Morales-Delgado, "Electrical circuits RC, LC, RL described by Atangana-Baleanu fractional derivatives", Int. J. Circuit Theory and Appl., DOI: 10.1002/cta.2348, 2017.
- [10] R. Zhou, D. Chen, "Fractional-Order 2xn RLC circuit network", Journal of Circuits, Systems, and Computers, vol. 24, pp. 1-25, 2015.
- [11] A.G. Radwan, M. E. Fouda, "Optimization of fractional-order RLC filters", Circuits, Systems, and Signal Processing, vol. 32, pp. 2097-2118, 2013.
- [12] J. Walczak and A. Jukobowska, "Resonance in series fractional order  $RL_{\beta}C_{\alpha}$  circuit, Electronics Review, vol. 4, pp. 210-213, 2014.
- [13] A.J. Cizek, J. Walczak, "Analysis of the transient state in a parallel circuit of the class  $RL_{\beta}C_{\alpha}$ ", Applied Mathematics and Computation, vol. 319, pp. 287-300, 2018.